Plant, Cell and Environment (2001) **24**, 65–76

Hydraulic architecture and water flow in growing grass tillers (*Festuca arundinacea* Schreb.)

P. MARTRE,[1] H. COCHARD[2] & J.-L. DURAND[1]

[1]*Unité d'Ecophysiologie des Plantes Fourragères, Institut National de la Recherche Agronomique, F-86 600 Lusignan, France,* [2]*Unité de Physiologie Intégrée des Arbres Fruitiers, Institut National de la Recherche Agronomique, F-63 039 Clermont-Ferrand, France*

ABSTRACT

The water relations and hydraulic architecture of growing grass tillers (*Festuca arundinacea* Schreb.) are reported. Evaporative flux density, E (mmol s^{-1} m^{-2}), of individual leaf blades was measured gravimetrically by covering or excision of entire leaf blades. Values of E were similar for mature and elongating leaf blades, averaging 2·4 mmol s^{-1} m^{-2}. Measured axial hydraulic conductivity, K_h (mmol s^{-1} mm MPa^{-1}), of excised leaf segments was three times lower than theoretical hydraulic conductivity (K_t) calculated using the Poiseuille equation and measurements of vessel number and diameter. K_t was corrected (K_t*) to account for the discrepancy between K_h and K_t and for immature xylem in the basal expanding region of elongating leaves. From base to tip of mature leaves the pattern of K_t* was bell-shaped with a maximum near the sheath–blade joint (≈ 19 mmol s^{-1} mm MPa^{-1}). In elongating leaves, immature xylem in the basal growing region led to a much lower K_t*. As the first metaxylem matured, K_t* increased by 10-fold. The hydraulic conductances of the whole root system, $L_{p_{root}}$ (mmol s^{-1} MPa^{-1}) and leaf blades, $L_{p_{blade}}$ (mmol s^{-1} MPa^{-1}) were measured by a vacuum induced water flow technique. $L_{p_{root}}$ and $L_{p_{blade}}$ were linearly related to the leaf area downstream. Approximately 65% of the resistance to water flow within the plant resided in the leaf blade. An electric-analogue computer model was used to calculate the leaf blade area-specific radial hydraulic conductivity, L_{p_r} (mmol s^{-1} m^{-2} MPa^{-1}), using $L_{p_{blade}}$, K_t* and water flux values. L_{p_r} values decreased with leaf age, from 21·2 mmol s^{-1} m^{-2} MPa^{-1} in rapidly elongating leaf to 7·2 mmol s^{-1} m^{-2} MPa^{-1} in mature leaf. Comparison of $L_{p_{blade}}$ and L_{p_r} values showed that ≈ 90% of the resistance to water flow within the blades resided in the liquid extra-vascular path. The same algorithm was then used to compute the xylem and extravascular water potential drop along the liquid water path in the plant under steady state conditions. Predicted and measured water potentials matched well. The hydraulic design of the mature leaf resulted in low and quite constant xylem water potential gradient (≈ 0·3 MPa m^{-1}) throughout the plant. Much of the water potential drop within mature leaves occurred within a tenth of millimetre in the blade, between the xylem vessels and the site of water evaporation within the mesophyll. In elongating leaves, the low K_t* in the basal growth zone dramatically increased the local xylem water potential gradient (≈ 2·0 MPa m^{-1}) there. In the leaf elongation zone the growth-induced water potential difference was ≈ 0·2 MPa.

Key-words: electric-circuit analogue; elongating leaf; hydraulic architecture; hydraulic conductivity; leaf transpiration; water relations.

Abbreviations: d_{water}^{dark}, local water deposition rate during the dark period; d_{water}^{light}, local water deposition rate during the light period (mmol mm^{-1} s^{-1}); E, evaporative flux density (mmol s^{-1} m^{-2}); EZ elongation zone; G_{dark}, average leaf elongation rate during the dark period (μm s^{-1}); G_{light}, average leaf elongation rate during the light period (μm s^{-1}). K_h, measured axial hydraulic conductivity of the xylem (mmol s^{-1} mm MPa^{-1}); k_t, theoretical axial hydraulic conductivity of individual vessels (mmol s^{-1} mm MPa^{-1}). K_t, theoretical axial hydraulic conductivity of all functioning parallel vessels (mmol s^{-1} mm MPa^{-1}); K_t*, theoretical axial hydraulic conductivity, corrected on the basis of the K_h/K_t ratio (mmol s^{-1} mm MPa^{-1}); $L_{p_{px}}$, radial hydraulic conductance of vessel cell walls for water flow from the protoxylem in the elongation zone to the surrounding expanding cells (mmol s^{-1} mm^{-2} MPa^{-1}); $L_{p_{blade}}$, total hydraulic conductance of the leaf blade (mmol s^{-1} MPa^{-1}); $L_{p_{blade}}^{A_l}$, total hydraulic conductance of the leaf blade normalized by the projected leaf blade surface area (mmol s^{-1} m^{-2} MPa^{-1}); L_{p_r}, radial hydraulic conductance of the extravascular liquid pathway for water flow from vessels to the evaporation site in the leaf blade, normalized by the projected leaf blade surface area (mmol s^{-1} m^{-2} MPa^{-1}); $L_{p_{root}}$, total hydraulic conductance of the entire root system (mmol s^{-1} MPa^{-1}); $L_{p_{root}}^{A_{pl}}$, hydraulic conductance of the entire root system, normalized by the projected leaf blade surface area of the plant (mmol s^{-1} m^{-2} MPa^{-1}); η, viscosity of water (MPa s^{-1}); q, water flow (mmol s^{-1}); P_x, xylem pressure (MPa); P_{sat}, vacuum pressure at which the slope of vacuum pressure versus flow rate relationship changed (MPa); Ψ_0, water potential at the excised end of the leaf in the vacuum-

Correspondence: J-L. Durand. Fax: + 33 5 49 55 60 68; E-mail: jldurand@lusignan.inra.fr

induced water flow experiments (MPa); Ψ_{sol}, water potential of solution (MPa); Ψ_{surf}, water potential of the evaporation site in the leaf blade in the vacuum induced water flow experiments; Ψ_l and Ψ_r, water potential of transpiring leaf and root, respectively (MPa); Ψ_{ez}, water potential of the elongation zone of leaf three (MPa); T, Transpiration rate (μmol s^{-1}).

INTRODUCTION

Transpiration is a necessary consequence of a plant's need to maintain rapid gas exchange in leaves and to transport nutrients and growth regulators throughout the plant. Because of resistance to the flow of water within a plant, the water flux produced by transpiration and osmotic gradients can lead to considerable reductions in tissue water potential (Denmead & Millar 1976; Wei, Tyree & Steudle 1999). Cell expansion is especially responsive to plant water status (Frensch 1997). Therefore, knowledge of the water potential distribution within plants is needed to understand the response of growth to plant water balance.

Under steady state conditions, the Ohm's law analogue of water flow in plants predicts that the drop in water potential, $\Delta\Psi$ (MPa), through a plant part of hydraulic conductivity, K_h (mmol s^{-1} m MPa^{-1}), and of length, Δx (m), is a function of water flow, q (mmol s^{-1}), as follows:

$$\Delta\Psi = -\frac{q}{K_h}\cdot\Delta x \qquad (1)$$

The xylem sap tension at a particular location in a plant will then depend: (*i*) on the soil water potential; (*ii*) on the sum of the resistances along the flow pathway from the soil to that point; and (*iii*) the water fluxes through each organ. It is therefore necessary to describe the 'hydraulic architecture' of a plant in order to understand the distribution of Ψ in its organs and assess the impact of this Ψ on growth.

The hydraulic architecture of woody plants has received more attention (e.g. Tyree 1988; Tyree & Ewers 1991; Cochard, Peiffer & Granier 1997) than that of herbaceous species, which remain virtually unstudied at a whole plant level. To our knowledge, the work of Meinzer *et al*. (1992) on *Saccharum officinarum* is the only published study of herbaceous hydraulic architecture on the whole plant scale, but radial water flow along the lamina was not assessed. The main objective of our study was to describe the hydraulic architecture of tillers of *Festuca arundinacea* Schreb. (tall fescue), a widely cultivated perennial grass.

The basal expanding region of growing leaves of tall fescue is a hydraulic bottleneck that might restrict axial water flow to the mature part of the blades and also through the expanding tissues (Martre, Durand & Cochard 2000). Although, the liquid resistances in the plant generally do not regulate the transpiration directly they may influence transpiration, as well as leaf growth, indirectly through their effect on leaf water potential and stomatal conductance (Tyree & Ewers 1991). Tall fescue is an anisohydric species, and poorly regulates its stomatal conductance (Ghashghaie & Saugier 1989; Thomas 1994; Durand *et al*. 1997). Thus the importance of the conductivity of liquid pathways in regulating plant water status and physiology could be critical for that species. Although most of the water moving through the xylem is lost through transpiration, a fraction is used in cell enlargement. The rate at which water is extracted from the transpiration stream to sustain expansive growth depends on the water potential of the xylem, the growth-induced water potential of the expanding cells and the conductivity between the two compartments. Hence, changes in the transpiration rate may affect the water status of the growth zone (Westgate & Boyer 1984). A thorough description of the hydraulic architecture of growing tillers should provide a useful tool for understanding the interactions between leaf growth and plant water status.

The first step in our study was to measure hydraulic conductivity of all the parts of tall fescue tillers. Two types of conductivities were considered: (*i*) axial conductivity through the xylem conduits; and (*ii*) extra-xylary radial conductivity, from the xylem vessels to site of evaporation within the mesophyll. Axial conductivities can be measured gravimetrically (K_h) or derived from anatomical measurements (K_t) assuming that xylem elements behave as ideal capillaries (Poiseuille's law). This assumption is rarely verified so K_t values need to be corrected (Gibson, Calkin & Nobel 1985; Hargrave *et al*. 1994). There are only a few detailed studies on plant organs in which both axial and radial hydraulic conductivity have been measured, but all have supported the generally accepted hypothesis that, under nonlimiting water supply, axial hydraulic conductivity in mature tissue is much greater than radial hydraulic conductivity. Many of the results come from research on roots (e.g. Frensch & Steudle 1989; North & Nobel 1991; Melchior & Steudle 1993), with leaves receiving less attention (Boyer 1977; Tyree & Cheung 1977).

The second step in our study was to measure the transpiration rates, T (μmol s^{-1}), of the different leaves. It was essential to measure T for elongating leaves because their own transpiration was likely to have a large impact on cell enlargement in the basal growth zone. The hydraulic conductivities and transpiration rates were used in a computer electric analogue model to compute xylem tension, P_x (MPa), blade water potential, Ψ_l (MPa), and expanding-cell water potential, Ψ_{ez} (MPa), along each leaf with high spatial resolution. We compared the Ψ-values predicted by our hydraulic architecture-based model with measurements of Ψ at different locations along the sap pathway.

MATERIALS AND METHODS

Plant material and growth conditions

All experiments were carried out using the same clone of tall fescue (*Festuca arundinacea* Schreb. cv. Clarine). A single parent plant was vegetatively propagated in a controlled-environment cabinet. Tillers were separated, roots removed, shoots cut to 70 mm, and the tillers were then

transferred to hydroponic culture using a nutrient solution described by Maurice, Gastal & Durand (1997). All measurements were made from days 14–21 after the plants were transferred to hydroponic solution, when the third leaf (L_3) that appeared following transfer was 200 ± 10 mm long (i.e. approximately 50% of its final length). At this stage, the ligule of L_3 was within 1 mm of the leaf base. L_3 was the last leaf to emerge from the enclosing older leaf sheath. The leaves which were one and two phyllochrons older were referred to as L_2 and L_1, respectively. To further standardize the leaf population, only tillers whose L_1 sheath lengths were similar (100 ± 5 mm) were selected.

In the controlled environment cabinet, the PPFD was 530 ± 10 μmol m^{-2} s^{-1} (provided by HQI-400 W/D lamps, Osram, München, Germany) during the 14 h of photoperiod. Relative humidity was controlled at 85 ± 2% throughout the 24 h light period, and air temperature was set at 18/24 °C (light/dark) in order to ensure a constant temperature (24 ± 0·5 °C) within the leaf elongation zone (*EZ*). Temperature of the growth zone was measured by inserting a fine thermocouple vertically through the ligule of L_1 to the *EZ* of L_3 of matched tillers (Onillon 1993).

Transpiration

Plant transpiration, T (mmol s^{-1}), was measured gravimetrically with an electronic balance (model LP1200S, Sartorius Corp, Bohemia, NY, USA, 10^{-3} g resolution) interfaced with a personal computer. The plants were placed in cylindrical vessels filled with aerated nutrient solution. Evaporation was prevented by adding 1 cm of paraffin oil at the surface of the nutrient solution. The weight was measured at intervals of 30 s. Running means over 10 min were calculated to reduce the noise in the output signal of the balance. T was calculated from these filtered values using a numerical differentiation formula based on third degree fitting of polynomials to five points equally spaced with intervals of 10 points (Erickson 1976).

The plants were transferred to the measurement growth chamber 2 d before the beginning of an experiment, and axillary tillers (two to three) were removed. The PPFD was 380 ± 10 μmol m^{-2} s^{-1} (provided by HQI-T 400 W D^{-1} lamps, Osram, München, Germany) during the 14 h light period. Relative humidity was decreased to 55/45 ± 10% (light/dark) in order to ensure contrasted dark/light conditions. Air temperature was maintained at 16·5/23 °C (light/dark) in order to provide a constant temperature (24 ± 0·5 °C) within the leaf growth zone. The plants were set on the balance at the end of a light period, at least 15 h prior to the manipulation of the plant transpiration.

To determine individual leaf contribution to the transpiration of tillers, the surface areas were manipulated, either by excising entire leaf blades or by sealing entire leaf blades in polyethylene film and tin foil. Transpiration of individual leaf blades was calculated as the difference between plant transpiration before (≥ 3 h) and after (≥ 3 h) the manipulations.

Leaf elongation rate

The elongation of L_3 was recorded concurrently with the water flux, on the same plant, using a linear variable differential transducer (LVDT L-50, Chauvin Arnoux, Paris, France). The tip of L_3 was attached by a thread to a metal arm leading to the core of the LVDT. The metal arm was counterbalanced to apply a tensile force of 7 g to the leaf to keep it straight. Leaf tip displacement was recorded on a datalogger (CR-10X, Campbell Scientific LTD, Leicestershire, UK) every 30 s. Data were smoothed and leaf elongation rate, G (μm s^{-1}), was computed using the same procedure as for T.

Leaf water potential

Once transpiration and leaf elongation measurements were done, leaf blades were sampled to measure their water potential, Ψ_l (MPa). Each lamina was covered on each side with self-adhesive tape, cut at about 100 mm from the apical tip and immediately stored in an insulated polyethylene bag lined with a damp tissue. Leaves were inserted into a Scholander-type pressure bomb, in which the chamber was lined with wet paper tissue, and the balancing pressure was recorded (Boyer 1995). Water potential measurements were taken within 5 min of collection. Previous experiments showed no significant changes in Ψ of the sealed leaf segment during that period compared to a leaf measured immediately. After the balance pressure was determined, leaf area was measured using a leaf area meter (model LI-3100 Area Meter, Li-Cor Inc., Lincoln, NE, USA).

Root system and sheaths bases were inserted into another plastic bag and immediately stored in a humid box to minimize errors due to water loss from the sample after excision. Several root segments and one leaf segment, taken at 20 mm from the base of L_3 (i.e. at the location of most active elongation), all 5 mm long, were cut with a razor blade in the humid box and rapidly sealed in thermocouple psychrometer chambers (model C-52, Wescor Inc., Logan, UT, USA). Water potential was measured in dew-point mode using a Wescor HR-33T microvoltmeter after a 3-h equilibration period, at 20 ± 0·1 °C in a temperature-controlled box.

Length of the elongation zone

The length of the elongation zone at the base of the leaf was determined by pricking holes every 5 mm from the base to 60 mm from the leaf base through the sheath of mature leaves using a fine entomologist's needle (0·2 mm diameter). Pricking was performed 4 h and sampling 10 h after the start of the 10 h dark period. Hole spacing was compared using a graduated ocular, and the distal end of the elongation zone was determined as being the point at which no further difference in spacing could be observed. The leaf elongation observed between pricking and sampling represented 8–15% of the length of the elongation zone.

Leaf axial hydraulic conductivity

Theoretical leaf axial hydraulic conductivities (K_t) were derived from xylem anatomical measurements. Five representative tillers were selected, excised at the root–shoot junction, and thin free-hand cross-sections were obtained with a razor blade at 5 mm intervals along the L_1 sheath (which enclosed the basal growing part of L_2 and L_3), and at 30 and 20 mm intervals for the emerged parts of the L_1 and L_2 blades, respectively. The lumen diameters of all vessels were measured under a fluorescent microscope at a magnification of 400× as described by Martre *et al*. (2000).

The theoretical axial hydraulic conductivity, K_t (mmol s^{-1} mm MPa^{-1}), of each cross section was calculated as the sum of the conductivity values of all the vessels (in parallel) in the section, assuming they were elliptical, using the equation proposed by Lewis & Boose (1995):

$$k_t = \frac{\pi}{64 \cdot \eta} \frac{a^3 \cdot b^3}{a^2 + b^2} \quad (2)$$

where η is the viscosity of water, and a and b are the diameters of the major and minor axes, respectively.

Actual hydraulic conductivities of L_1 blade segments were measured using the technique described by Sperry, Donnelly & Tyree (1988) as adapted to grass leaves by Martre *et al*. (2000). In short, leaves were cut under water at the blade joint, kept under water, cut again into 30 mm long segments and longitudinally wrapped around an aluminium bar covered with Teroson (sticky putty). Leaf segments around the bar were then covered with Teflon tape and fitted at both ends into silicon tubing filled with a solution of degassed 0·1% (v/v) concentrated HCl (37·7%) solution (*c.* pH 2) filtered through a 0·2 μm filter. This low pH inhibited microbial growth within the tubing system, that could lead to clogging of the xylem during conductance measurements (Sperry *et al*. 1988). Tests have shown no influence of this solution on hydraulic conductance compared with distilled water or 10 mM citric acid solution. Each tubing end led to a reservoir of HCl solution; one reservoir was placed on an analytical balance interfaced with a computer, while the other was elevated to create a hydrostatic pressure head of 6 kPa. The rate of solution flow to the reservoir situated on the balance was measured over five successive 30 s intervals. K_h was computed as the flow rate (mmol s^{-1}) divided by the pressure gradient (MPa m^{-1}). Using an 0·1% (w/v) alcian blue solution, it was possible to check that water flowed only within the vessels and not through the extracellular air spaces during these measurements. After K_h measurements were completed, K_t values were estimated, as before, for each segment.

Total hydraulic conductance of emerged leaf blades

Leaf blades of L_1 were cut under water at the blade joint. Leaf blades of L_2 and L_3 were cut 6 cm under the blade joint of L_1 in order to calculate the hydraulic conductance of the entire emerged part of these blades. The excised leaves were fitted via Exacanal tubing to a supply of degassed HCl solution, leading to an analytical balance as described above. As for K_h measurement, tests have shown no influence of this solution on hydraulic conductance of the blade or root system compared with distilled water or 10 mM citric acid. Blades were then wrapped loosely with damp cloth to prevent the blade surface from drying out, and were inserted into a vacuum canister, which could be sealed and linked to a vacuum pump as described by Kolb, Sperry & Lamont (1996). The canister was made with an opaque cylindrical PVC pipe sealed at one end by a PVC cap and at the other by a removable PVC lid. The lid had an opening allowing the proximal end of the sample to protrude. An air-tight seal between the blade and the PVC lid was achieved by fitting the blade in a rubber stopper. About 1 cm of the blade or sheath was covered with damp cloth and left outside the canister to equilibrate the intercellular air space with atmospheric pressure thereby preventing water from flooding the extracellular spaces, at least at low vacuum pressure.

After the canister was sealed, the flow rate at zero pressure was measured until it stabilized. Vacuum pressure steps of 0·008 MPa were then applied within 20 s and kept constant until a new constant flow rate was established. Flow rate was then recorded over five successive 30 s intervals. Flow rate stabilization took about 30 min at 0·008 MPa, but only 5–10 min at the higher vacuum pressure. After stabilization, constant flow rates could be recorded for at least 4 h. After measurements were completed, the surface area of the blade in the canister was measured using a leaf area meter.

The vacuum pressure in the canister was equal to the water potential of the liquid–vapour interface in the leaf, and therefore represented the driving force for the movement of water from the water reservoir to the evaporating sites in the blade. Therefore it was appropriate to use this pressure difference to calculate the hydraulic conductance of the leaf. Total hydraulic conductance of the leaf blade, $L_{p_{blade}}$ (mmol s^{-1} MPa^{-1}), was calculated as the slope of the relationship between vacuum pressure and flow rate. Values of $L_{p_{blade}}$ were corrected for the leaf segment outside the canister, assuming that there was only axial water flow through this segment, in series with the leaf blade inside the canister. The axial conductance of the leaf segment outside the canister was about 5% of the corrected leaf blade hydraulic conductance.

Total hydraulic conductance of entire root system

At the vegetative state the internode measured only ≈ 1 mm, thus the root system cut at the root–shoot junction could not be sealed in the tubing without any leaks. Root conductance was therefore measured on plants cut at 60 mm from the root–shoot junction (i.e. 60 mm from the base of L_1 sheath). Axillary tillers were cut under water at their base, and the cut surfaces were sealed with hydrophilic low viscosity vinyl polysiloxane (Reprosil, Dentsply Inter-

national Inc., Milford, DE, USA). The shoot base was cut under water 60 mm above the root–shoot junction, kept under water, covered with Teflon tape and fitted via silicon tubing to an HCl solution supply as described above. The root system was wrapped loosely in a damp cloth and inserted into the vacuum canister, and the hydraulic conductance of the root system was measured as described for blades. After measurements were completed, the fresh weight of the root system was determined and then oven dried at 70 °C for 48 h to determine the dry weight.

Root hydraulic conductance, $L_{p_{root}}$ (mmol s^{-1} MPa^{-1}) was corrected for the shoot part outside the canister, assuming that the leaf bases were in parallel with each other, that all were in series with the roots, and that there was only axial water flow through the leaf bases. The root hydraulic conductance values included the resistance of internodes and nodes, which were around 2 mm long in total. The axial conductance of the leaf bases was around 30% of the corrected root hydraulic conductance.

Statistical analyses

Student *t*-tests were used to test the differences in the slope of the regression lines for $L_{p_{blade}}$ and $L_{p_{root}}$ versus leaf area, and to compare *E*-values, Ψ, and blade area of L_1, L_2 and L_3. Statistical significance of difference was considered to be $P < 0{\cdot}05$.

RESULTS

Transpiration, water potential and leaf elongation rate

The transpiration rates of the different leaf blades were measured by successive defoliation or by covering entire leaf blades. As both types of manipulation gave similar results, the results were combined. There was a close linear relationship between *T* for individual leaves or whole tillers and leaf surface area (Fig. 1). *E* was not significantly different for the different leaf blades ($P > 0{\cdot}05$) and averaged 2·4 mmol m^{-2} s^{-1} (Table 1). Transpiration of the sheaths, measured while all blades were covered, was virtually zero (data not shown).

Water potential measured for transpiring leaves was about 50% and 30% higher (less negative) for L_3 and L_2 growing leaves, respectively, compared to that of L_1 mature leaves (Table 1). The water potential of the elongation zone (Ψ_{ez}) was – 0·44 ± 0·02 MPa, and the bulk root water potential (Ψ_r) – 0·17 ± 0·03 MPa (Table 1).

Average leaf elongation rate was about 40% higher during the night than during the light period (Table 1).

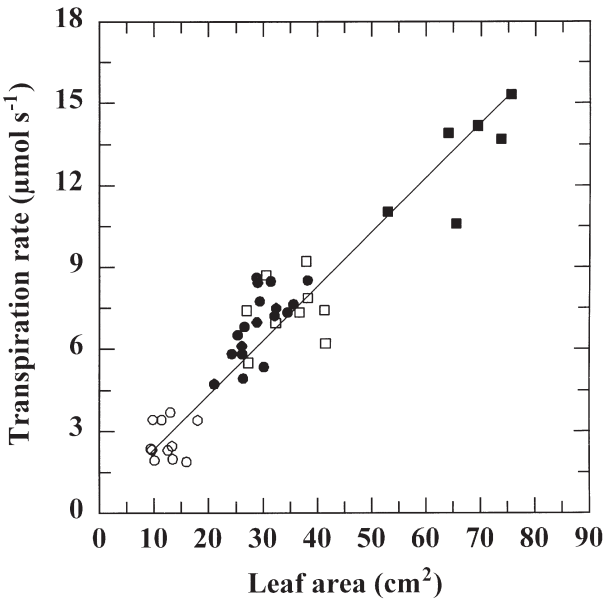

Figure 1. Relationship between transpiration rates and leaf area for whole tall fescue plants (■) and leaf blades L_1 (●), L_2 (□), and L_3 (○). (—), linear regression ($y = 0{\cdot}20x + 0{\cdot}35$, $r = 0{\cdot}94$, $P < 0{\cdot}05$).

Axial hydraulic conductivity

In L_1 leaf blades, K_h values, derived from measured flow rates and pressure gradients, ranged between 4 and 29 mmol s^{-1} mm MPa^{-1} (Fig. 2). The relationship between K_h and K_t predicted from vessel lumen diameters using the Poiseuille equation was not linear, as the K_t/K_h ratio increased slightly for large vessel diameters, and K_t was about three times K_h. Aerenchyma in the sheath made measurement of K_h impossible using our gravimetric technique,

		Leaf		
	Root	L_1	L_2	L_3
Blade area (cm^2)	–	32·30 ± 1·66[a]	36·6 ± 2·64[a]	12·4 ± 0·87[b]
E (mmol m^{-2} s^{-1})	–	2·67 ± 0·17[a]	2·31 ± 0·32[a]	2·21 ± 0·22[a]
EZ length (mm)	–	–	27·1 ± 1·8[a]	32·7 ± 1·0[b]
G_{dark} (μm s^{-1})	–	–	–	0·54 ± 0·06
G_{light} (μm s^{-1})	–	–	–	0·38 ± 0·03
Ψ_{ez} (MPa)	–	–	–	– 0·44 ± 0·02
Ψ_l (MPa)	–	– 0·80 ± 0·09[a]	– 0·63 ± 0·05[a,b]	– 0·54 ± 0·08[b]
Ψ_r (MPa)	– 0·17 ± 0·03	–	–	–

Table 1. Dimension, growth rates and water status of the three visible leaves of single tillers of tall fescue in controlled environment. Leaf blade area, evaporative flux density (*E*), transpiring leaf blades (Ψ_l), L_3 elongation zone (Ψ_{ez}) and root (Ψ_r) water potential, average elongation rates of L_3 during the dark (G_{dark}) and the light (G_{light}) periods of the diurnal cycle, and the length of the elongation zone (*EZ*) for L_2 and L_3. Data are means ± SE for $n = 10$–12. Means in the same line with different superscripts are significantly different at $P < 0{\cdot}05$ from Student *t*-test

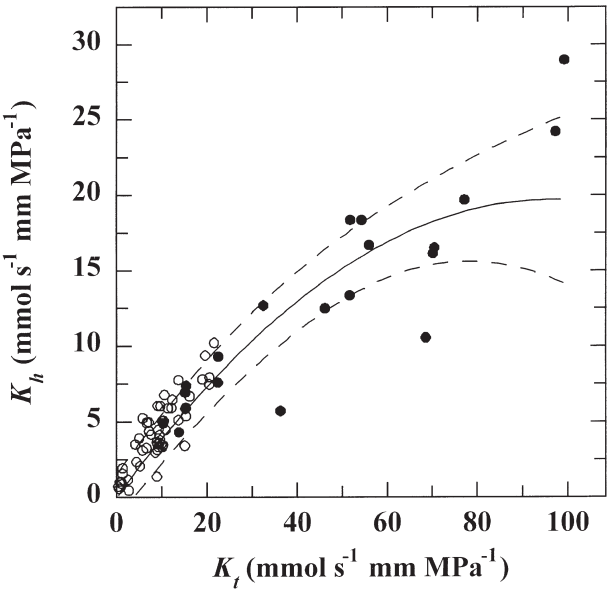

Figure 2. The relationship between theoretical (K_t, predicted from Poiseuille equation for ideal capillaries) and measured (K_h) axial hydraulic conductivity of tall fescue mature leaf blades (●). Each point represents a single leaf segment whereas K_t was computed from measurements of individual vessel diameter, in cross-sections taken from the middle of the segment where K_h was previously measured. All fluorescent protoxylem and large metaxylem vessels within each cross-section were measured. Points for L_3 (○) are reproduced from Martre *et al*. (2000). **(—)**, nonlinear regression for L_1 and L_3 ($y = (-0{\cdot}0021x + 0{\cdot}40)x$, $r = 0{\cdot}92, P < 0{\cdot}05$). (- - -), 95% confidence intervals.

because these air spaces became water-filled and conducted much of the water under pressure.

In L_1, K_t* increased substantially along the sheath from 1·9 ± 0·6 mmol s^{-1} mm MPa^{-1} at the leaf sheath base to 19·7 ± 1·8 mmol s^{-1} mm MPa^{-1} near the blade joint (Fig. 3). K_t decreased to the same extent along the blade. Along the region exposed to light (i.e. above 100 mm from the base), K_t* values of L_2 blades were close to those for the L_1 blades. In the blade of L_1, measured K_h were highly consistent with both L_1 and L_2 K_t*, which indicated that the two batches of plants were comparable. Given the similarities in plant material and growth conditions, the pattern of xylem maturation in L_3 studied in detail by Martre *et al*. (2000) was used here: (i) within the growth zone, only the protoxylem vessels were conductive; (ii) the proportion of functional large metaxylem increased linearly from 0 at a distance of 60 mm from leaf base to 1 at a distance of 100 mm from leaf base, i.e. where the leaf tissues emerged from the sheath of L_2. For L_2, it was assumed that the pattern of xylem maturation was the same as in L_3. In the basal 75 mm of L_2, K_t* differed greatly from that for L_1 because of the large proportion of nonfunctional large metaxylem vessels in the immature tissues. It has been shown that the location of the first lignified metaxylem vessels is closely correlated with the length of the elongation zone in *Avena sativa* (Goodwin 1942) and *Glycine max* (Paolillo & Rubin 1991). Thus, the assumption concerning the pattern of xylem maturation in L_2 would not result in an error greater than 5 mm, since the length of the elongation zone of L_2 was only 5 mm shorter than that of L_3 (see Table 1).

The K_t and K_h values were similar for the tips of L_3, L_2, and L_1 (Fig. 3). Hence, L_3, L_2, and L_1 represent three stages of leaf development and provide a temporal description of the development of hydraulic architecture in a single leaf.

Total hydraulic conductance of emerged leaf blades

Pressure–flow lines for typical vacuum experiments are presented in Fig. 4(a). The water flux at 0 MPa was close to zero (Fig. 4a inset). For L_1 and L_2, the relationship between flow rate and pressure could be represented by two lines with different slopes. The pressure at which the slope changed (P_{sat}) was, in all trials, between 0·016 and 0·024 MPa. When the slope changed, the mesophyll became hyaline and flooded with water. For L_3, however, the relationship was adequately described by a single line (Fig. 4a).

A single linear relation held between $L_{p_{blade}}$ and the leaf

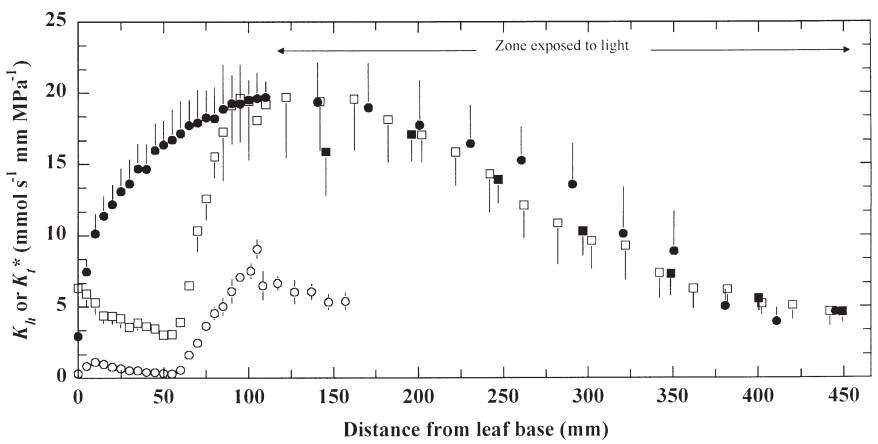

Figure 3. Measured axial hydraulic conductivity of the xylem (K_h, ■) for L_1 and corrected theoretical axial hydraulic conductivity (K_t*) as a function of distance from the base for the tall fescue leaves L_1 (●), L_2 (□), and L_3 (○). K_h was measured for 30 mm long segments. L_1, L_2, and L_3 leaves for K_t* computation were taken from the same tillers, see text for details of K_t* computation. Data are means ± SE (represented by vertical bars, except when smaller than the symbol) for $n = 5$–8. Points from L_3 were taken from Martre *et al*. (2000).

area in the canister for L_1 and L_2 (Fig. 5). In contrast, $L_{p_{blade}}$ for L_3 was weakly related to leaf surface area.

To compare the conductance of the different organs, the slope of the pressure–flow line was divided by the projected evaporative surface area downstream of the organ, i.e. leaf blade surface area in the canister. The initial $L_{p_{blade}}^{A_1}$ values for L_1 and L_2 were 6·6 ± 0·7 and 8·9 ± 0·8 mmol s^{-1} m^{-2} MPa^{-1} and increased by 25 and eight fold above P_{sat}, respectively (Table 2). The average $L_{p_{blade}}^{A_1}$ value for L_3 was 19·6 ± 2·9 mmol s^{-1} m^{-2} MPa^{-1}, and it doubled above P_{sat}.

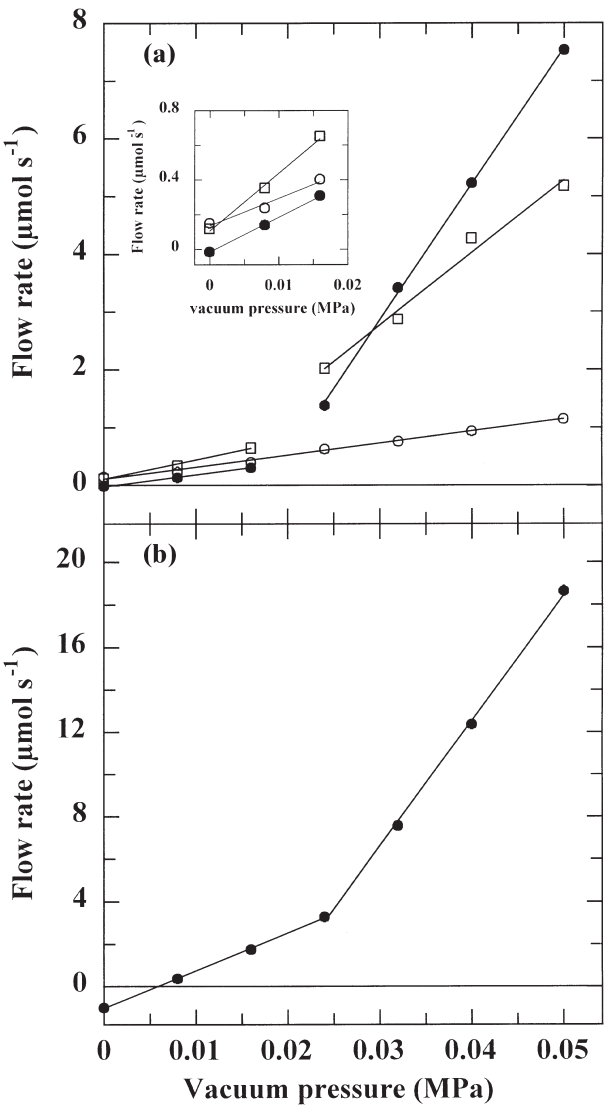

Figure 4. Representative plots of vacuum pressure and the corresponding flow rate measured for: (a) single leaf blades L_1 (●), L_2 (□) and L_3 (○); and (b) an entire root system of tall fescue. Each point is a flow rate for a given vacuum pressure. The slope is equal to the hydraulic conductance. Inset in (a), close-up of flow rate at the lowest pressures.

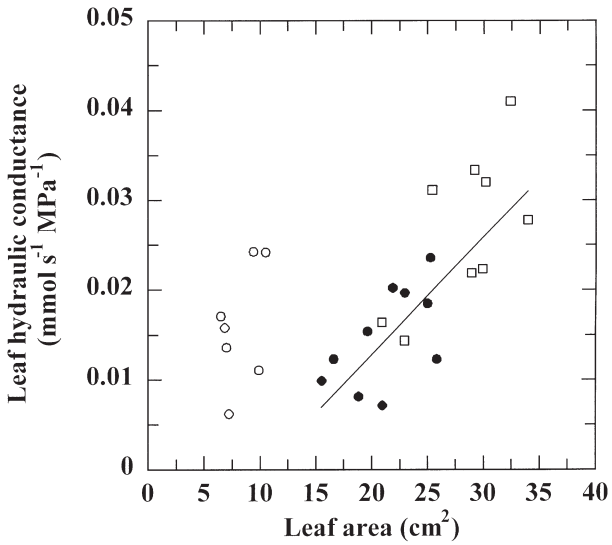

Figure 5. The relationship between hydraulic conductance and the leaf blade area for L_1 (●), L_2 (□), and L_3 (○). Each point represents a separate leaf blade. (**—**), linear regression for L_1 and L_2 ($y = 0{\cdot}0013x + 0{\cdot}013$, $r = 0{\cdot}80$).

Total hydraulic conductance of entire root systems

In all experiments with roots, the initial flow rate was negative (Fig. 4b), indicating that the root was losing water in the direction of the solution reservoir, i.e. that root pressure was higher than atmospheric pressure. The magnitude of the water flux at 0 MPa ranged from – 1 to – 3 μmol s^{-1}. The vacuum pressure at which the slope changed was more variable (between 0·016 and 0·04 MPa) from one root system to another than for leaf blades.

$L_{p_{root}}$ was closely related to the leaf surface area of the plant, but not to root fresh weight (Fig. 6). As root fresh weight was closely correlated to root dry weight (data not shown), $L_{p_{root}}$ was not related to root dry weight, either. Similarly to $L_{p_{blade}}^{A_1}$, the tiller root specific conductance ($L_{p_{root}}^{A_{p1}}$), was computed by dividing $L_{p_{root}}$ by the tiller leaf area. Initial $L_{p_{root}}^{A_{p1}}$ value was 12·27 ± 0·71 mmol s^{-1} m^{-2} MPa^{-1}, but after P_{sat} the values increased by about five times (Table 2).

DISCUSSION

Since the same relation between transpiration and leaf area held for individual leaves and whole tillers (Fig. 1), leaf blade excision or covering did not seem to alter the transpiration of the remaining transpiring blades, contrary to what has been found in *Saccharum* spp. (Meinzer & Grantz 1990) and *Pennisetum typhoides* and *Arachis hypogaea* (Black & Squire 1979). This discrepancy with previous works may be due to the smaller size of tall fescue tillers, specifically the number of leaves and the stem length, which reduced variations in the stem water potential while the transpiring leaf area was reduced. Moreover, the ability of

	$L_{p_{blade}}^{A_1}$ or $L_{p_{root}}^{A_{p1}}$ (mmol s^{-1} m^{-2} MPa^{-1})		L_{p_r} (mmol s^{-1} m^{-2} MPa^{-1})	$\frac{L_{p_{blade}}^{A_1}}{L_{p_r}}$
	0 MPa to P_{sat}	above P_{sat}	0·92	
L_1 blade	6·6 ± 0·7[a]	152·2 ± 18·0[d]	7·2 ± 0·8[a]	0·92
L_2 blade	8·9 ± 0·8[b]	64·9 ± 16·2[e]	10·35 ± 1·0[b]	0·86
L_3 blade	19·6 ± 7·0[c,f]	34·0 ± 8·6[c,f]	21·2 ± 7·9[c,f]	0·92
Root	12·3 ± 0·7[f]	59·1 ± 8·1[g]	–	–

Table 2. Conductances of the leaves and roots of tall fescue tillers grown on nutrient solution in controlled environment. Entire root system hydraulic conductance ($L_{p_{root}}^{A_{p1}}$), and total ($L_{p_{blade}}^{A_1}$) and radial (L_{p_r}) leaf blade hydraulic conductance of tall fescue. The conductances are normalized by the projected leaf surface area. Values of $L_{p_{root}}^{A_{p1}}$ and $L_{p_{blade}}^{A_1}$ are reported before (0 MPa to P_{sat}) and after (above P_{sat}) the change of slope of the relationship between flow rate and vacuum pressure. $\frac{L_{p_{blade}}^{A_1}}{L_{p_r}}$: ratio between total and radial conductance. Data are means ± SE for n = 8–11. Means with different superscripts were significantly different at $P < 0.05$ using a Student's t-test

tall fescue to regulate its stomatal conductance is low (Ghashghaie & Saugier 1989; Thomas 1994).

We have not found any published measurement of E of elongating grass leaves. So far it was generally considered to be very low because elongating leaves are vertical and still partially rolled. In the present experiment however, E for L_2 and L_3 elongating leaves was rather strikingly close to that of L_1 mature leaf (Table 1).

Poiseuille's equation has been used widely to predict conductivity in the xylem. Results, however, have been variable, with measured conductivity and flows ranging from 20 to 100% of theoretical values (e.g. Dimond 1966; Calkin, Gibson & Nobel. 1986; Hargrave *et al*. 1994). In tall fescue, measured conductivity was only 20% of the theoretical value (Fig. 2). The discrepancy between K_h and K_t might be due to the short vessel length and the low conductance of the pit membrane.

During vacuum-driven flow experiments, a rapid increase in leaf blade conductance was found above a pressure (P_{sat}) consistently ranging from 0·016 to 0·024 MPa (Fig. 4). The blade then turned hyaline and dye uptake confirmed that the intracellular air spaces became filled with water (data not shown). According to Jurin's law, this threshold pressure would correspond to a pore diameter of ≈ 15 μm, which was consistent with our observations of the average size of intercellular air spaces (data not shown). In roots, P_{sat} was more variable (between 0·016 and 0·04 MPa), but the same conclusion could be drawn (Passioura 1988). As a consequence, the hydraulic conductance established at pressures lower than P_{sat} was considered to be the true conductance.

The $L_{p_{blade}}^{A_1}$ values for L_1 (Table 2) were consistent with those found for mature blades of tall fescue, in pressure efflux experiments (≈ 5·5 mmol s^{-1} m^{-2} MPa^{-1}; Stroshine *et al*. 1985) and for *Prunus persica* leaves (Améglio *et al*. 1998). But it was 50% less than that of *Glycine max*, *Gossypium hirsutum*, *Citrus paradisi*, and *Persea americana* leaves, which range from 2·9 to 4·3 mmol s^{-1} m^{-2} MPa^{-1} (Moreshet *et al*. 1990).

The hydraulic conductance of the root system was weakly related to root fresh or dry weight (Fig. 6a). This might be due to the fact that $L_{p_{root}}$ was not constant along the root (Sanderson, Whitbread & Clarkson 1988; Frensch & Steudle 1989). However, $L_{p_{root}}$ was closely related to the whole plant leaf area (Fig. 6b). As discussed in detail by Tyree, Velez & Dalling (1998), scaling $L_{p_{root}}$ to leaf surface area provides an estimate of the intrinsic efficiency of the root system in supplying water to leaves, making it possible to compare absolute root conductance and leaf conductance. The $L_{p_{blade}}^{A_1} / L_{p_{root}}^{A_{p1}}$ ratio was about 0·6 (Table 2). This indicates that 65% of the resistance within the plant was located within the blade. This is higher than that reported by Black (1979) for *Helianthus annuus*, where approximately half of the total plant resistance to water flow is located within the root, and a further 30% within the lamina.

Whole leaf conductance ($L_{p_{blade}}$) corresponds to the total conductance of a network which includes axial conductances in series and radial conductances in parallel. In this study, the axial conductance was measured (K_h) or estimated (K_t*). Assuming that the leaf-specific radial hydraulic conductance of the blade, L_{p_r} (mmol s^{-1} m^{-2} MPa^{-1}), was constant along the blade (Fig. 5), it was possible to compute L_{p_r} from $L_{p_{blade}}^{A_1}$ and K_t* measurements numerically. For this purpose, blades representative of L_1, L_2 and L_3 were segmented into 5 mm long segments with axial and radial conductances of K_t* and L_{p_r}, respectively (Fig. 7). A computer simulation based on the algorithm developed by Tyree (1988) for the dynamic solution of water flow in tree was used to solve for flow and water potential across the network of conductors. Each conductance was assigned an arbitrary capacity, set at 50 mmol m^{-2} MPa^{-1}. The programme performed nonsteady state computations by iteration until the rate of water flow into the leaf equalled the rate of water flow out of the leaf, which was the condition that defined the conservative flux. The model was run so as to take into account boundary condi-

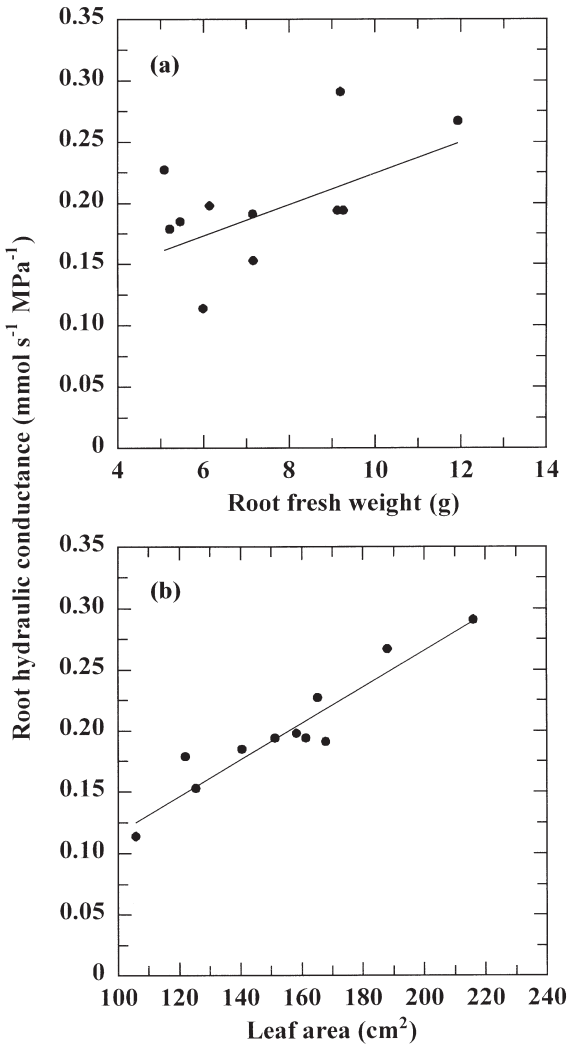

Figure 6. The relationship between hydraulic conductance of entire root systems and (a) total root fresh weight; and (b) total leaf area of tall fescue plants. Each point represents a separate root system. Lines, linear regressions (in *a*, $y = 0{\cdot}012x + 0{\cdot}09$, $r = 0{\cdot}55$, *n*.s.; and in b, $y = 0{\cdot}0015x + 0{\cdot}032$, $r = 0{\cdot}942$, $P < 0{\cdot}05$).

tions representative of a leaf measured in a vacuum canister. Water potential at the leaf base was set at 0 MPa, and water potential at the liquid–vapour interface, within the mesophyll air spaces, was set equal to the vacuum pressure in the canister (0·016 MPa). L_{p_r} was initially set at an arbitrary value close to $L_{p_{blade}}^{A_1}$ for L_1 and gradually increased until the observed flow rate was obtained.

The calculated values of L_{p_r} for L_1, L_2, and L_3 were 7·2 ± 0·8, 10·3 ± 1·0, and 21·2 ± 7·9 mmol s^{-1} m^{-2} MPa^{-1}, respectively (Table 2). Given the flooding of the extracellular air space at the beginning of $L_{p_{blade}}$ measurements in L_3, the L_{p_r} of those leaves was probably overestimated. The average $L_{p_{blade}}^{A_1}/L_{p_r}$ ratio was 0·90 ± 0·02 (Table 2), which indicated that most of the resistance within the blade was located in the radial extraxylary pathway. This is consistent with the results of Tyree & Cheung (1977), who also found that over 90% of the hydraulic resistance in the leaf blades of *Fagus grandifolia* trees lay in the liquid extraxylary pathway. However, Wei *et al*. (1999), using the high-pressure flow-meter technique in *Zea mays* leaves, found that the radial extraxylary resistance represents only 30% of the total leaf blade hydraulic resistance.

The same simulation approach as for calculation of L_{p_r} was used to compute the water potentials at different points in the hydraulic network for a transpiring tiller. The electric analogue model of the tiller with three leaves is shown in Fig. 8. Each of the three leaves was divided into 5 mm long elements and assigned a radial and axial conductance. No radial conductance was assigned to the sheaths of L_1 and L_2 as their transpiration and elongation rates were close to zero. A single conductor represented the zone of insertion of roots and leaves. The total number of 5 mm long elements was 399. In each leaf segment, the axial conductivity was set at the relevant K_t* (Fig. 3) or L_{p_r} (Table 2). As the value for L_3 was probably overestimated, the L_{p_r} of L_2, which is also a growing leaf, was used instead. The radial conductance associated with the growth sustaining water flux in the elongation zone of L_3 ($L_{p_{ps}}$ = 6·5 mmol s^{-1} m^{-2} MPa^{-1}, normalized by the surface area of protoxylem wall) calculated by Martre *et al*. (2000) was used here. This resulted in radial conductance along the growth zone varying with the total perimeter of the protoxylem.

Input variables were: (i) Ψ_{sol} (0 MPa); (ii) E (Table 1) and leaf segment width; and (iii) the growth sustaining water flux in the elongation zone of L_3. Given the low elongation rate of L_2, the radial flux in the growth zone of L_2 was set at zero. As the water flux associated with growth is negligible compared to the flux associated with transpiration, thus considering the growth associated flux of L_2 as zero did not significantly modify the xylem water potential of L_2.

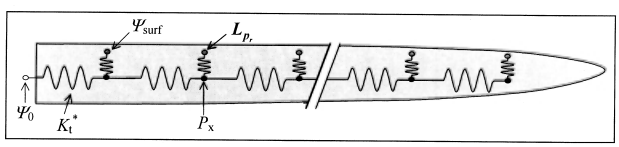

Figure 7. Simplified diagram of the electrical analogue used to compute L_{p_r} for tall fescue leaf blades. The blade was divided into 5 mm long segments. Axial water flow occurred along the axial conductors, K_t*, connected in series. Radial water flow occurred along the radial conductors, L_{p_r}, connected in parallel at the end of each axial element. The water potentials were Ψ_0 at the basal end of the blade, P_x at the end of an axial conductor, and Ψ_{surf} at the end of a radial conductor (representing the site of water evaporation in the 'mesophyll'). Each axial conductor was 5 mm long, and the radial conductors had a surface area that varied along the blade according to the blade shape. Each conductor was assigned an arbitrary capacitance value set at 50 mmol m^{-2} MPa^{-1}. Ψ_0 and Ψ_{surf} were given as boundary conditions, whereas the water outflow and P_x were unknown. The rate of evaporation from each radial element was represented by a constant current source, and is given by EA_i, where E was the evaporative flux density, and A_i was the surface area of the i^{th} radial element.

The radial flux from the protoxylem vessels to the surrounding expanding cells is equal to the local water deposition rate (d_{water} mmol mm^{-1} s^{-1}). In elongating leaves of tall fescue, the spatial distribution of water content within the elongation zone is almost steady during the dark and light period (Schnyder & Nelson 1988), and about 80% of the greater water deposition rate during darkness is explained by the dark stimulation of the leaf elongation rate. Therefore, light time d^{light}_{water} for L_3 was calculated as:

$$d^{light}_{water}(x) = d^{dark}_{water}(x) \cdot \frac{G_{light}}{G_{dark}} \quad (3)$$

where $d^{light}_{water}(x)$ was the water deposition rate at location x during the light period, $d^{dark}_{water}(x)$ was the water deposition rate at location x during the dark period, G_{light} was the average leaf elongation rate during the light period and G_{dark} was the average leaf elongation rate during the dark period. Previous results of $d^{dark}_{water}(x)$ and G_{dark} obtained with similar tall fescue tillers in the same experimental conditions (Martre *et al*. 2000) were used to compute $d^{light}_{water}(x)$ as a function of G_{light} measured in this study. The output variables were the total transpiration flux, the absorption flux, and the water potential of the xylem and extravascular tissues within each mapped segment.

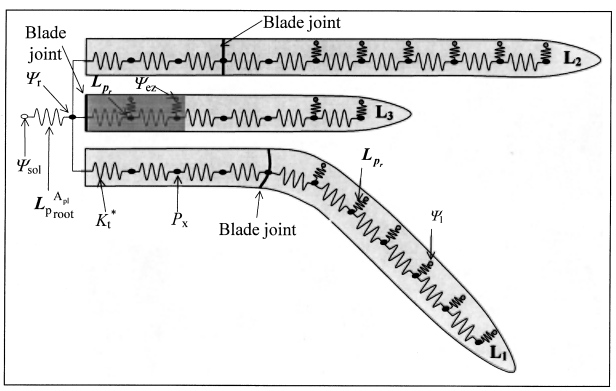

Figure 8. Simplified electric analogue representation of tall fescue hydraulic architecture used for water potential computations. The root was represented by a single conductor, $L_{P_{root}}^{A_{pl}}$, which included the node and internode resistances. Each of the three leaves was divided into 5 mm long conductors. Water was transported in the leaves through a set of axial conductors, K_t*, and in the emerged part of the blades, from the axial conductors (representing the xylem) to the evaporative sites, through a radial conductor, L_{p_r}. In the elongation zone (*EZ*) of L_3 (shaded area of L_3) growth-associated flow occurred along radial conductor, $L_{p_{px}}$. The water potentials were Ψ_{sol} at the root surface, P_x at the end of a K_t* conductor, Ψ_r at the root-leaf junction, Ψ_l at the end of a L_{p_r} conductor, and Ψ_{ez} at the end of a $L_{p_{px}}$ conductor. Ψ_r, P_x, Ψ_{ez}, and Ψ_l were unknown and Ψ_{sol} was given as boundary condition. $E.A_i$ gave the rate of evaporation from each radial element, where E was the evaporative flux density, and A_i was the surface area of the i^{th} radial element.

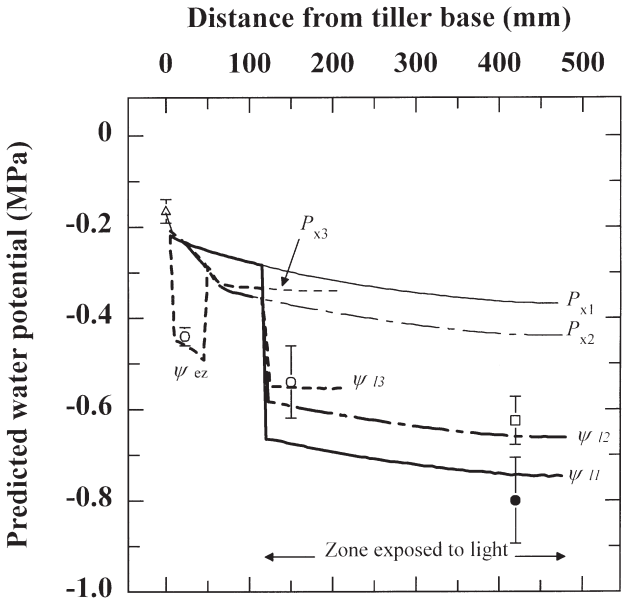

Figure 9. Computed profiles of xylem pressure and extravascular water potential versus distance from tiller base for tall fescue leaves L_1 (—), L_2 (– – –), and L_3 (- - -), as predicted from root system and leaf axial and radial hydraulic conductances, leaf transpiration and elongation rates. Xylem water potential (P_x), fine lines. Extra-vascular water potential (Ψ_l), thick lines. See text for details of the computation method. Measured values of water potential of roots (△), L_1 (●), L_2 (□), and L_3 (○) are reported for comparison (means ± SE, n = 10–12).

The predicted water potential values were within 10% of the actual values measured with the pressure chamber or the psychrometer (Fig. 9). The predicted xylem water potential gradient along L_1 was relatively modest (0·3 MPa m^{-1}) and almost constant. In contrast, the low K_t* in the basal region of the L_2 and L_3 leaves resulted in a much higher P_x gradient from the base of the leaf to 65 mm (2·0 MPa m^{-1}). Above 65 mm, the P_x gradient was low and essentially constant (0·2 MPa m^{-1}), similar to what was computed for L_1. This confirms that the basal region of elongating leaves is a hydraulic constriction that restricts axial water movement (Martre *et al*. 2000). In transpiring regions of the leaves, the model predicted large (up to 0·3 MPa) and rather constant radial water potential differences between the xylem vessels and the surrounding tissues. Indeed, the leaf water potentials measured using a pressure chamber were within 10% of the predicted values, indicating that such measurements reflected mainly the mesophyll water potential. This was expected as the volume of water in the xylem is small compared to the bulk of water in the leaf. Hence, about 40% of the drop in water potential within the plant occurred radially in the blade along a distance of only a few tenths of millimetres. This is consistent with the results of Melcher *et al*. (1998) for transpiring *Zea mays* and *Saccharum officinarum* leaves. The Ψ_l difference between the sheath–blade joint and tip was small

(< 0·08 MPa), as was also found by Slatyer (1967), who measured in the field a drop in water potential of 0·2–0·3 MPa along a *Pennisetum americanum* lamina 70 cm long in the field.

Overall, the hydraulic architecture of the tall fescue leaf thus revealed properties similar to the hydraulic architecture of a tree species (e.g. Cochard *et al*. 1997), where the branch leaf area and K_h are adjusted in such a way that leaf water potential remains nearly constant along the trunk. The measured water potential in the growth zone was – 0·44 ± 0·02 MPa (Table 1), i.e. very close to the computed values (Fig. 9). Onillon (1993) measured similar values at noon in well fertilized and irrigated tall fescue plants in the field. However, our values were 0·1 MPa lower than those found by Martre, Bogeat-Triboulot & Durand (1999) in the elongation zone of nontranspiring leaves of similar tillers measured using a cell pressure probe. The lower values of Ψ_{ez} found here were associated with a lower osmotic water potential (data not shown), whereas the turgor was not significantly different from that found using the pressure probe (≈ 0·5 MPa). Thus, this decrease in Ψ_{ez} appeared to be related to an osmotic adjustment of the growing cells while the plant transpired, rather than to a relaxation of the growing cell wall during the measurement of the water potential of excised tissues. In spite of the osmotic adjustment in the growing cells, the predicted growth-induced water potential difference between the xylem and the surrounding expanding cells was close to 0·2 MPa, which was 0·1 MPa smaller than for non-transpiring leaves (Martre *et al*. 1999).This reduction in water availability for cell enlargement could be the primary cause of the slower leaf elongation rate while the plant transpires, as shown for *Zea mays* leaves (Westgate & Boyer 1984) and *Glycine max* hypocotyls (Nonami & Boyer 1993).

ACKNOWLEDGMENTS

We wish to acknowledge Dr B. Moulia (INRA, Lusignan, France) for offering invaluable suggestions and stimulating discussions during the course of this work, Dr G.B. North (Occidental College, Los Angeles, CA, USA) for correcting the manuscript, and Mrs L. Cousson, Mr P. Poussot, Mr G. Millet and Mr C. de Berranger for excellent technical assistance. P.M. was supported by a grant from INRA and the Région Poitou-Charentes. H.C. thanks Dr M.T. Tyree (USDA, Burlington, VT, USA) for sharing the code of his programme.

REFERENCES

Améglio T., Cochard H., Picon C. & Cohen M. (1998) Water relations and hydraulic architecture of peach trees under drought conditions. *Acta Horticulturea* **465,** 355–361.

Black C.R. (1979) The relative magnitude of the partial resistances to transpirational water movement in sunflower (*Helianthus annuus* L.). *Journal of Experimental Botany* **30,** 245–253.

Black C.R. & Squire G.R. (1979) Effects of atmospheric saturation deficit on the stomatal conductance of pearl millet (*Pennisetum typhoides* S. & H.) and groundnut (*Arachis hypogaea* L.). *Journal of Experimental Botany* **30,** 169–181.

Boyer J.S. (1977) Regulation of water movement in whole plants. In *Integration of Activity in the Higher Plant*, Vol. 31 (ed. H.D. Jennings), pp. 455–470. Symposia of the society for experimental biology, Cambridge.

Boyer J.S. (1995). *Measuring the Water Status of Plants and Soils*. Academic Press, San Diego.

Calkin H.W., Gibson A.C. & Nobel P.S. (1986) Biophysical model of xylem conductance in tracheids of the fern *Ptersi vittata*. *Journal of Experimental Botany* **37,** 1054–4064.

Cochard H., Peiffer M., Le Gall K. & Granier A. (1997) Developmental control of xylem hydraulic resistances and vulnerability to embolism in *Fraxinus excelsior* L.: impacts on water relations. *Journal of Experimental Botany* **48,** 655–663.

Denmead O.T. & Millar B.D. (1976) Water transport in wheat plants in the field. *Agronomy Journal* **68,** 297–303.

Dimond A.E. (1966) Pressure and flow relations in vascular bundles of the tomato plant. *Plant Physiology* **441,** 119–131.

Durand J.L., Gastal F., Etchebest S., Bonnet A.C. & Ghesquière M. (1997) Interspecific variability of plant water status and leaf morphogenesis in temperate forage grasses under water deficit. *European Journal of Agronomy* **7,** 99–107.

Erickson R.O. (1976) Modeling of plant growth. *Annual Review of Plant Physiology* **27,** 407–434.

Frensch J. (1997) Primary responses of root and leaf elongation to water deficits in the atmosphere and soil solution. *Journal of Experimental Botany* **48,** 985–999.

Frensch J. & Steudle E. (1989) Axial and radial hydraulic resistance to roots of maize (*Zea mays* L.). *Plant Physiology* **91,** 719–726.

Ghashghaie J. & Saugier B. (1989) Effects of nitrogen deficiency on leaf photosynthetic response of tall fescue to water deficit. *Plant, Cell and Environment* **12,** 261–271.

Gibson A.C., Calkin H.W. & Nobel P.S. (1985) Hydraulic conductance and xylem structure in tracheid-bearing plants. *International Association of Wood Anatomists Bulletin* **6,** 293–302.

Goodwin R.H. (1942) On the development of xylary elements in the first internode of *Avena* in dark and light. *American Journal of Botany* **29,** 818–828.

Hargrave K.R., Kolb K.J., Ewers F.W. & Davis S.D. (1994) Conduit diameter and drought-induced embolism in *Salvia mellifera* greene. *New Phytologist* **126,** 695–705.

Kolb K.J., Sperry J.S. & Lamont B.B. (1996) A method for measuring xylem hydraulic conductance and embolism in entire root and shoot systems. *Journal of Experimental Botany* **47,** 1805–1810.

Lewis A.M. & Boose E.R. (1995) Estimating volume flow rates through xylem conduits. *American Journal of Botany* **82,** 1112–1116.

Martre P., Bogeat-Triboulot M.B. & Durand J.L. (1999) Measurement of a growth-induced water potential gradient in tall fescue leaves. *New Phytologist* **142,** 435–439.

Martre P., Durand J.L. & Cochard H. (2000) Changes in axial hydraulic conductivity along elongating leaf blades in relation to xylem maturation in tall fescue. *New Phytologist* **146,** 235–247.

Maurice I., Gastal F. & Durand J.L. (1997) Generation of form and associated mass deposition during leaf development in grasses: a kinematics approach for non-steady growth. *Annals of Botany* **80,** 673–683.

Meinzer F.C., Goldstein G., Neufeld H.S., Grantz D.A. & Crisosta G.M. (1992) Hydraulic architecture of sugarcane in relation to patterns of water use during plant development. *Plant, Cell and Environment* **15,** 471–477.

Meinzer F.C. & Grantz D.A. (1990) Stomatal and hydraulic conductance in growing sugarcane: stomatal adjustment to water transport capacity. *Plant, Cell and Environment* **13,** 383–388.

Melcher P.J., Meinzer F.C., Yount D.E., Goldstein G. & Zimmermann U. (1998) Comparative measurements of xylem pressure in transpiring and non-transpiring leaves by means of the pressure chamber and the xylem pressure probe. *Journal of Experimental Botany* **49,** 1757–1760.

Melchior W. & Steudle E. (1993) Water transport in onion (*Allium cepa* L.) roots. Changes in axial and radial hydraulic conductivities during root development. *Plant Physiology* **101,** 1305–1315.

Moreshet S., Huck M.G., Hesketh J.D. & Peters D.B. (1990) Relationships between sap flow and hydraulic conductivity in soybean plants. *Agronomie* **10,** 381–389.

Nonami H. & Boyer J.S. (1993) Direct demonstration of growth-induced water potential gradient. *Plant Physiology* **102,** 12–19.

North G.B. & Nobel P.S. (1991) Changes in hydraulic conductivity and anatomy caused by drying and rewetting roots of. *Agave Deserti (Agavaceae). American Journal of Botany* **78,** 906–915.

Onillon B. (1993) Effet d'une contrainte hydrique édaphique sur la croissance de la fétuque élevée soumise à différents niveaux de nutrition azotée. Etude à l'échelle foliaire et à celle du couvert végétal. PhD Thesis. Université de Poitiers, France.

Paolillo D.J. & Rubin G. (1991) Relative elemental rates of elongation and the protoxylem-metaxylem transition in hypocotyls of soybean seedlings. *American Journal of Botany* **78,** 845–854.

Passioura J.B. (1988) Water transport in and to roots. *Annual Review of Plant Physiology and Plant Molecular Biology* **39,** 245–265.

Sanderson J., Whitbread F.C. & Clarkson D.T. (1988) Persistent xylem cross-walls reduce the axial hydraulic conductivity in the apical 20 cm of barley seminal root axes: implications for the driving force for water movement. *Plant, Cell and Environment* **11,** 247–256.

Schnyder H. & Nelson C.J. (1988) Diurnal growth of tall fescue leaf blades. I. Spatial distribution of growth, deposition of water, and assimilate import in the elongation zone. *Plant Physiology* **86,** 1070–1076.

Slatyer R.O. (1967) *Plant–Water Relationships*, pp. 282–285. Academic Press, New York.

Sperry J.S., Donnelly J.R. & Tyree M.T. (1988) A method for measuring hydraulic conductivity and embolism in xylem. *Plant, Cell and Environment* **11,** 35–40.

Stroshine R.L., Rand R.H., Cooke J.R., Cutler J.M. & Chabot J.F. (1985) An analysis of resistance to water flow through wheat and tall fescue leaves during pressure chamber efflux experiments. *Plant, Cell and Environment* **8,** 7–18.

Thomas H. (1994) Diversity between and within temperate forage grass species in drought resistance, water use and related physiological responses. *Aspects of Applied Biology* **38,** 47–55.

Tyree M.T. (1988) A dynamic model for water flow in a single tree: evidence that models must account for hydraulic architecture. *Tree Physiology* **4,** 195–217.

Tyree M.T. & Cheung Y.N.S. (1977) Resistance to water flow in *Fagus grandifolia* leaves. *Canadian Journal of Botany* **55,** 2591–2599.

Tyree M.T. & Ewers F.W. (1991) The hydraulic architecture of trees and other woody plants. *New Phytologist* **119,** 345–360.

Tyree M.T., Velez V. & Dalling J.W. (1998) Growth dynamics of root and shoot hydraulic conductance in seedlings of five neotropical tree species: scaling to show possible adaptation to differing light regimes. *Oecologia* **11,** 293–298.

Wei C., Tyree M.T. & Steudle E. (1999) Direct measurement of xylem pressure in leaves of intact maize plants: a test of the cohesion-tension theory taken account of hydraulic architecture. *Plant Physiology* **121,** 1191–1205.

Westgate M.E. & Boyer J.S. (1984) Transpiration- and growth-induced water potentials in maize. *Plant Physiology* **74,** 882–889.

Received 9 April 2000; received in revised form 18 August 2000; accepted for publication 18 August 2000